

# Theoretical and experimental analysis of H<sub>2</sub> binding in a prototype metal organic framework material

Lingzhu Kong,<sup>1</sup> Valentino R. Cooper,<sup>1,2</sup> Nour Nijem,<sup>3</sup> Kunhao Li,<sup>4</sup> Jing Li,<sup>4</sup> Yves J. Chabal,<sup>3</sup> and David C. Langreth<sup>1</sup>

<sup>1</sup>*Department of Physics and Astronomy, Rutgers University, Piscataway, New Jersey 08854-8019*

<sup>2</sup>*Materials Science and Technology Division, Oak Ridge National Laboratory, Oak Ridge, Tennessee 37831-6114\**

<sup>3</sup>*Department of Materials Science and Engineering,  
University of Texas at Dallas, Richardson, Texas 75080*

<sup>4</sup>*Department of Chemistry and Chemical Biology,  
Rutgers University, Piscataway, New Jersey 08854-8087*

Hydrogen adsorption by the metal organic framework (MOF) structure Zn<sub>2</sub>(BDC)<sub>2</sub>(TED) is investigated using a combination of experimental and theoretical methods. By use of the nonempirical van der Waals density-functional (vdW-DF) approach, it is found that the locus of deepest H<sub>2</sub> binding positions lies within two types of narrow channel. The energies of the most stable binding sites, as well as the number of such binding sites, are consistent with the values obtained from experimental adsorption isotherms and heat of adsorption data. Calculations of the shift of the H–H stretch frequency when adsorbed in the MOF give a value of approximately  $-30\text{ cm}^{-1}$  at the strongest binding point in each of the two channels. Ambient temperature infrared absorption spectroscopy measurements give a hydrogen peak centered at  $4120\text{ cm}^{-1}$ , implying a shift consistent with the theoretical calculations.

Hydrogen storage technology is one bottleneck for the utilization of hydrogen as an energy source for mobile applications. Metal-organic frameworks (MOFs) comprise a rather new class of porous materials in which metal ions or clusters are linked by organic units [1]. The scaffold structure and large apparent surface area make these materials potential candidates for hydrogen storage applications. One such material, MOF-5, was shown to adsorb 1.3 wt.-% of hydrogen at 77 K and 1 atm [2]. A recent effort with Zn<sub>2</sub>(BDC)<sub>2</sub>(TED) reported an uptake of 2.1 wt.-% [3]. Here BDC is benzenedicarboxylate (C<sub>8</sub>H<sub>4</sub>O<sub>4</sub>) and TED is triethylenediamine (C<sub>6</sub>H<sub>12</sub>N<sub>2</sub>). To rationally design or modify MOF structures to meet storage needs, it is critical to understand the interaction between the MOF matrix and the adsorbed hydrogen molecules. Furthermore, the quest to understand the physisorption and possible dissociative chemisorption of H<sub>2</sub> within a MOF is a fascinating problem in its own right. In the present letter, we show how a relatively recently developed nonempirical theoretical method [4, 5] and infrared absorption measurements [6] can be combined with isotherm and heat of adsorption data [3] to obtain a detailed picture of the adsorption of H<sub>2</sub> in MOFs. For this purpose we use Zn<sub>2</sub>(BDC)<sub>2</sub>(TED) [3] as a prototype.

Spectroscopic and theoretical studies have confirmed that H<sub>2</sub> is weakly bound in MOFs and the binding is mainly from long-range dispersive interactions [7]. The nonlocal electron correlation in this type of interaction makes accurate and efficient electronic structure calculations very difficult. Quantum chemical methods that account for these interactions typically scale poorly with system size and are limited to only fragments of the true MOF structure. On the other hand, ordinary density functional theory (DFT) methods, which are efficient and scale well with system size, fail to reproduce the correct

behavior of the van der Waals interactions, which are important in these systems [8]. For example, an H<sub>2</sub> binding energy of 21.7 meV was obtained for the main H<sub>2</sub> adsorption sites in MOF-5 by use of the generalized gradient approximation (GGA) within DFT [9], while the experimental value is 49–54 meV [10].

An alternative, a van der Waals density functional (vdW-DF), has been developed by our group and collaborators [4, 5]. It incorporates the van der Waals interaction into a fully nonlocal and nonempirical density functional for the correlation energy, which retains ordinary DFT's good description of covalent bonding. The method has been successfully applied to various sparse systems [4, 5, 11]. Here we begin by benchmarking vdW-DF on the binding of H<sub>2</sub> to an isolated BDC linker, where there exist calculations via well established quantum chemical methods [12, 13]. It is found that H<sub>2</sub> binds most strongly when pointed along the symmetrically placed axis through the center of the benzene ring, and sitting a distance a little over 3 Å away with a binding energy of approximately 4 kJ/mol. We find that while a standard GGA calculation using the PBE functional [14] fails to predict more than a third of the interaction energy, the vdW-DF [15] not only gives the correct binding energy, but quite well reproduces the whole binding curve [13] and the potential energy landscape [13], though, as is typical [4, 5, 11], the intermonomer equilibrium distance is slightly too large. In the full MOF, we find that this site's binding energy increases by 3 kJ/mol due to long range interactions with other parts of the MOF—a very nonlocal effect that cannot be reproduced by standard density functionals. More spectacularly this binding point of the fragment becomes only a saddle point in the potential energy surface of the MOF, showing that calculations on fragments alone do not nec-

essarily give relevant information about the binding sites in the full MOF, or even useful information as to where to look for them.

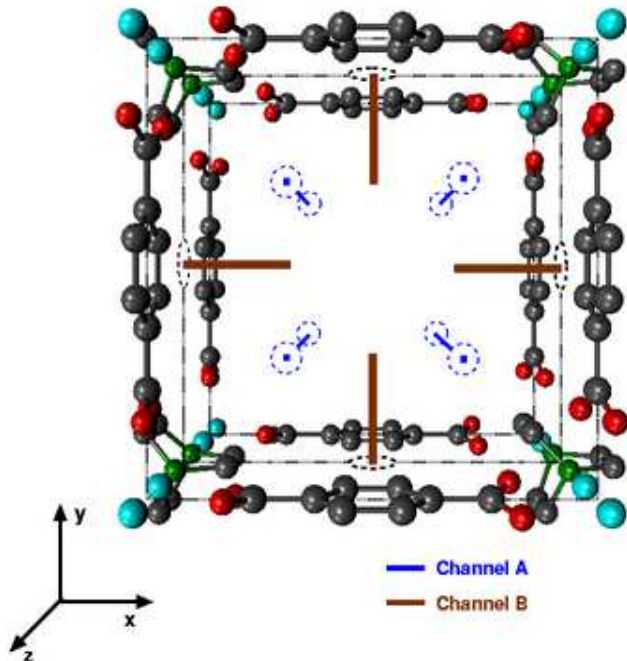


FIG. 1: A perspective top view of the unit cell of the MOF. The BDC linkers and the metal atoms are evident in this view, while the TED pillars are more clearly seen in the two subsequent figures. Atomic color scheme: black C, green N, red O, blue-green Zn; H atoms are not shown. The locations of Channels A (thin blue) and B (thick brown) are schematically indicated. The dashed circles indicate places where the respective channels continue into the adjoining unit cell.

The basic MOF structure was taken from experiment [3]. Based on the single crystal data of the guest-free structure [16], the C in TED and O in BDC have a 4-fold and 2-fold disorder, respectively. A simplified structure eliminating the disorder is used in the actual calculations [16], as shown in Fig. 1. The underlying Bravais lattice is tetragonal with  $a = b = 10.93 \text{ \AA}$  and  $c = 9.61 \text{ \AA}$ , with a basis consisting of one formula unit of  $\text{Zn}_2(\text{BDC})_2(\text{TED})$ . Our vdW-DF calculations found that the strong  $\text{H}_2$  binding regions are located in two types of channel (see Fig. 1). One such channel type runs in the  $c$  direction through the length of the crystal, with four such channels entering and leaving each unit cell. We denote these as Channels A. An energy contour map of one of them is shown in Fig. 2. These four channels are not quite equivalent in the calculated model because of the differing faces presented by the nearest TED and oxygen twist, but the differences are relatively small ( $\sim 1 \text{ kJ/mol}$ ). A second type of channel, which we refer to as Channel B, runs in the  $a$  or  $b$  direction. These run only from one unit cell (as we draw it here) to the next, because they would otherwise run through the center of the cell, which is a

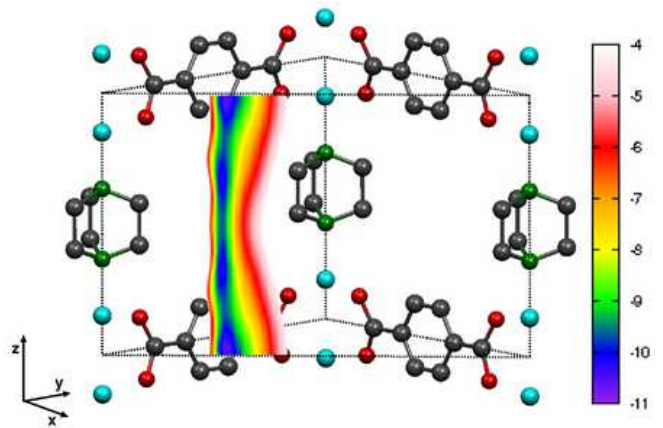


FIG. 2: A diagonal side view of half the unit cell, showing a contour energy map of one of the four instances of Channel A. The  $\text{H}_2$  molecule was aligned in the  $z$  direction. The units of the color scale are  $\text{kJ/mol}$ .

weak binding region. One of the halves of Channel B is illustrated in Fig. 3. There are four halves of Channel B per unit cell, i.e. two Channel B's per cell. What is clear from the the maps in the Figs. 2 and 3, is that the mean binding energy in the maximum regions is  $10 \text{ kJ/mol}$  in round numbers for each of the channels, with Channel B perhaps a little higher. Although the maximum binding energies in Channels B are affected only very slightly ( $\sim 0.2 \text{ kJ/mol}$ ) by the orientation of the nearest TED and oxygen components, the widths of these channels in the  $xy$  plane (not illustrated) are more strongly affected. It is interesting that unlike what is apparently true for some isorecticular MOFs (IRMOFs) [17], there is little binding specifically associated with the metal atoms or in their vicinity.

There are two caveats with respect to the predicted binding of  $\sim 10 \text{ kJ/mol}$ . First, the binding is dependent on the  $\text{H}_2$  orientation (see Table I), with a variation of  $\sim 1 \text{ kJ/mol}$ . Second, the channels are narrow, and  $\text{H}_2$  is a quantum mechanical object. Its ground state energy will be higher than the potential minimum. A full treatment is beyond the scope of this letter, but harmonic zero point energy estimates indicate that this effect could reduce the effective binding by 1 to 2  $\text{kJ/mol}$  per  $\text{H}_2$ .

The above results are consistent with the experimental  $\text{H}_2$  uptake curves at  $T = 77 \text{ K}$  and  $87 \text{ K}$  [3], which we found to be Langmuir isotherms to a high degree of accuracy. The Langmuir isotherm is simply a plot of a Fermi function against  $\exp(\mu/kT)$  ( $\mu$  is the chemical potential), combined with the realization that  $\exp(\mu/kT)$  is proportional to the pressure  $P$  outside the MOF. The fact that a single Langmuir isotherm (rather than a linear combination of them) fits the uptake data implies that the important adsorption sites all have about the same binding energy, just as we find. The experimental binding energy can be determined both from the isotherm fit

and independent heat of adsorption measurements [3]: each give a value of  $\sim 7$  kJ/mol. When the quantum corrections mentioned above as well as thermal excitations involving them are accurately calculated and applied, we expect that our well-bottom value of  $\sim 10$  kJ/mol will be significantly reduced and closer to experiment. Finally, our fit to the Langmuir isotherms gives  $\sim 13$  adsorption sites per unit cell. An inspection of Figs. 2 and 3 implies a total of 12, provided that we assign two per unit cell to each of the 4 Channels A per cell, and 1 to each of the Channel B halves. More importantly, the magnitude of the interaction energy increases approximately linearly as we load hydrogen molecules on these sites one by one.

We now turn to the calculation of the  $H_2$  stretch frequencies. We carried out a series of calculations varying the bond length of  $H_2$ , with the center of  $H_2$  and the host atoms fixed at their equilibrium positions. The resulting potential energy curve for each configuration was used in the Schrödinger equation to obtain the eigenvalues and excitation frequencies [18]. At each of the two minimum positions, we performed the calculations for all three molecular orientations along  $x$ ,  $y$ , and  $z$ . For the Channel A minimum, we calculated the stretching frequency along the body-center diagonal as well. We express our results in terms of the shifts from our calculated value of the frequency for free  $H_2$  of  $4160\text{ cm}^{-1}$ . Although the latter is accidentally more accurate than expected for the level of approximation used, no use is made of this fact, and we consider only the frequency shift upon adsorption to be relevant for the comparison with experiment.

The vibrational frequency of the hydrogen molecule shifts downward when absorbed into the MOF matrix,

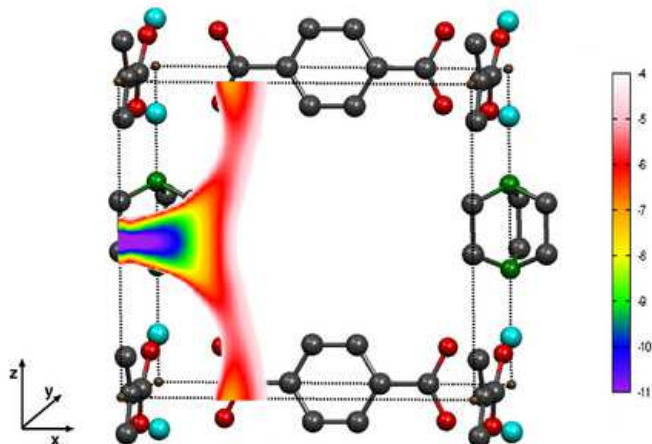


FIG. 3: A side view of half the unit cell, showing one of the four instances of Channel B, each of which extend an equal amount into the respective neighboring unit cell. The contour map color scale and the  $H_2$  orientation are the same as for Fig. 2.

as shown in Table I. The relative change from the free  $H_2$  value, is mainly due to the van der Waals interaction, which is weak. The shifts predicted by an application of the GGA were found to be substantially smaller still. The shifts that we predicted with the vdW functional were  $-28\text{ cm}^{-1}$  and  $-25\text{ cm}^{-1}$  for the preferable binding orientations in Channels A and B respectively and are smaller in magnitude for other molecular orientations. The interaction energies for different orientations are within  $\sim 1$  kJ/mol for each channel, which indicates that all the orientations will be well populated at room temperature. Furthermore, the translational states, which have a range of frequencies of up to  $\sim 100\text{ cm}^{-1}$ , will be well occupied, implying gain and loss contributions of comparable amplitudes. As a result, we expect the frequency peak to be substantially broadened at such ambient temperatures.

TABLE I: Calculated vibrational frequency shifts and interaction energies for various orientations at the two types of binding site. The largest binding Channel A sites are at the intersections of that channel with the cell body diagonals (see Fig. 2), while those for Channel B are at the cell boundaries (see Fig. 3). The frequency shifts are relative to our calculated values for free  $H_2$  of  $4160\text{ cm}^{-1}$ .

	$H_2$ orientation	$\omega$ shift $\text{cm}^{-1}$	Energy (kJ/mol)
Channel A	diagonal	-28	-10.1
	x	-17	-9.1
	y	-21	-9.5
	z	-15	-8.7
Channel B	x	-25	-10.9
	y	-15	-9.6
	z	-4	-9.7

Infrared absorption spectroscopy is particularly useful for studying the incorporation of  $H_2$  molecules in semiconductors, as was demonstrated for amorphous silicon [6]. The onset of IR activity and the position of the  $H_2$  internal vibrational mode are both sensitive measures of  $H_2$  interaction with the matrix. The actual measurements are difficult because the absorption cross section of  $H_2$  is expected to be so weak that overtones and combination bands of the MOF material will interfere with the measurement.

For these experiments,  $Zn_2(BDC)_2(TED)$  powder samples were prepared solvothermally [3]. A small amount (10 mg) was lightly pressed on a KBr pellet, the constitutive solvent removed by activation (annealing for 10 h under  $10^{-2}$  Torr vacuum) and the spectrum was recorded (using a clean KBr pellet as reference). The top panel of Fig. 4 shows the spectrum associated with overtones and combination bands of the clean MOF. Upon loading with high pressure He gas, these bands are perturbed, as evidenced by spectral shifts, due to minor rearrangement of the organic ligands. Consequently, in order to obtain a clean spectrum of  $H_2$  molecular absorption,  $D_2$  molecules

were used as a background for the H<sub>2</sub> absorption experiments, as shown in the middle spectra in Fig. 4. The difference obtained is shown in the bottom three spectra for selected pressures (600, 700 and 800 psi).

The main observation is the presence of a well-defined band centered at 4120 cm<sup>-1</sup>, which is composed of 3/4 ortho and 1/4 para hydrogen (room temperature distribution), hence the asymmetry towards higher frequencies. The measured shift of -35 cm<sup>-1</sup> from the unperturbed ortho (4155 cm<sup>-1</sup>) and para (4161 cm<sup>-1</sup>) frequencies is in good agreement with the calculated -28/25 cm<sup>-1</sup> shifts. Furthermore, the integrated areas (measured from 300 to 800 psi) are linear with pressure, which is expected since, even at 800 psi, the average H<sub>2</sub> loading per unit cell is only ~1 H<sub>2</sub> out of ~12 possible sites, well within the linear regime for sequential loading found by the calculations. The observed vibrational band is ~54 cm<sup>-1</sup> broad, consistent with phonon and thermal broadening at room temperature, and with tails extending over 50 cm<sup>-1</sup>, which may arise from the translational states.

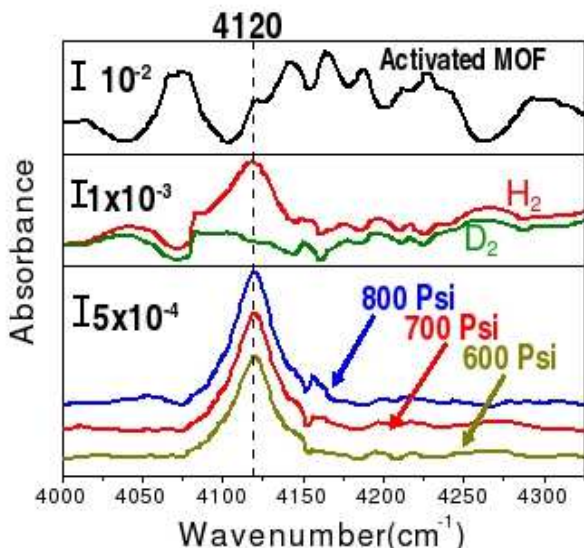


FIG. 4: Infrared absorbance of the Zn<sub>2</sub>(BDC)<sub>2</sub>(TED) MOF at room temperature. Top panel: clean MOF at ambient pressure; Middle panel: MOF at 800 psi of H<sub>2</sub> (upper curve) or D<sub>2</sub> (lower curve); Bottom panel: difference between the H<sub>2</sub> and D<sub>2</sub> spectra at several pressures.

To summarize, we have shown that a combination of experimental and theoretical methods gives a consistent and accurate picture of H<sub>2</sub> binding in a prototype MOF structure. This picture will become still more precise when both low temperature infrared absorption can be performed, and the calculations of quantum effects on the motion of H<sub>2</sub> within the MOF are complete. The methods are now ripe for application to larger MOF structures with larger H<sub>2</sub> binding energies and hopefully will give

additional clues about structural and chemical changes that can increase these energies even further.

Work supported by DOE-DE-FG02-08ER46491. Work by V.R.C. supported by NSF-DMR-0456937 at Rutgers until 9/15/08 and by DOE, Division of Materials Sciences and Engineering at ORNL after 9/15/08.

\* Permanent address for V.R.C. since 9/16/08.

- [1] M. Eddaoudi, D. B. Moler, H. Li, B. Chen, T. M. Reineke, M. O'Keeffe, O. M. Yaghi, *Acc. Chem. Res.* **34**, 319 (2001).
- [2] J. L. C. Rowsell, A. R. Millward, K. S. Park, O. M. Yaghi, *J. Am. Chem. Soc.* **126**, 5666 (2004).
- [3] J. Y. Lee, D. H. Olson, L. Pan, T. J. Emge, J. Li, *Adv. Func. Mater.* **17**, 1255 (2007).
- [4] M. Dion, H. Rydberg, E. Schröder, D. C. Langreth, and B. I. Lundqvist, *Phys. Rev. Lett.* **92**, 246401 (2004); Erratum: *Phys. Rev. Lett.* **95**, 109902 (2005).
- [5] T. Thonhauser, V. R. Cooper, Shen Li, A. Puzder, P. Hyldgaard, and D. C. Langreth, *Phys. Rev. B* **76**, 125112 (2007).
- [6] Y. J. Chabal and C. K. N. Patel, *Phys. Rev. Lett.* **53**, 210 (1984).
- [7] A. Centrone, D. Y. Siberio-Pérez, A. R. Millward, O. M. Yaghi, A. J. Matzger, and G. Zerbi, *Chem. Phys. Lett.* **411**, 516 (2005); A. Kuc, T. Heine, G. Seifert, and H. A. Duarte, *Chem. Eur. J.* **14**, 6597 (2008).
- [8] T. Heine, L. Zhechkov, and G. Seifert, *Phys. Chem. Chem. Phys.* **6**, 980 (2004).
- [9] T. Mueller and G. Ceder, *J. Phys. Chem. B* **109**, 17974 (2005).
- [10] Steven S. Kaye and Jeffrey R. Long, *J. Am. Chem. Soc.* **127**, 6506 (2005).
- [11] D. C. Langreth et al., *J. Phys. Cond. Mat.* (in press); J. Kleis, B. I. Lundqvist, D. C. Langreth, E. Schröder, *Phys. Rev. B* **76**, 100201(R) (2007); V. R. Cooper, T. Thonhauser, A. Puzder, E. Schröder, B. I. Lundqvist, and D. C. Langreth, *J. Am. Chem. Soc.* **130**, 1304 (2008).
- [12] O. Hübner, A. Glöss, M. Fichtner, and W. Klopfer, *J. Phys. Chem. A* **108**, 3019 (2004); T. Sagara, J. Klassen, and E. Ganz, *J. Chem. Phys.* **121**, 12543 (2004); C. Buda and B. D. Dunietz, *J. Phys. Chem. B* **110**, 10479 (2006).
- [13] T. Sagara, J. Klassen, and E. Ganz, *J. Chem. Phys.* **123**, 214707 (2005).
- [14] J. P. Perdew, K. Burke and M. Ernzerhof, *Phys. Rev. Lett.* **77**, 3865 (1996).
- [15] Troullier-Martins pseudopotentials were used [N. Troullier and J. M. Martins, *Phys. Rev. Lett.* **43**, 1993 (1991)] in a modified vdW version of the Abinit plane-wave code [X. Gonze, et al., *Comp. Mat. Sci.* **25**, 478 (2002)] with an energy cutoff of 50 Ry. A 60 Ry cutoff was used for the calculations summarized in Table I.
- [16] D. N. Dybtsev, H. Chun, and K. Kim, *Angew. Chem. Int. Ed.* **43**, 5033 (2004).
- [17] J. L. C. Rowsell, J. Eckert, and O. M. Yaghi, *J. Am. Chem. Soc.* **127**, 14904 (2005).
- [18] J. W. Cooley, *Math. Comput.* **15**, 363 (1961).